

Aalborg Universitet

Multi-objective Stochastic Planning of Electric Vehicle Charging Stations in Unbalanced Distribution Networks Supported by Smart Photovoltaic Inverters

Gholami, Khalil; Karimi, Shahram; Anvari-Moghaddam, Amjad

Published in: Sustainable Cities and Society

DOI (link to publication from Publisher): 10.1016/j.scs.2022.104029

Creative Commons License CC BY-NC-ND 4.0

Publication date: 2022

Document Version Accepted author manuscript, peer reviewed version

Link to publication from Aalborg University

Citation for published version (APA):

Gholami, K., Karimi, S., & Anvari-Moghaddam, A. (2022). Multi-objective Stochastic Planning of Electric Vehicle Charging Stations in Unbalanced Distribution Networks Supported by Smart Photovoltaic Inverters. Sustainable Cities and Society, 84, 1-14. Article 104029. https://doi.org/10.1016/j.scs.2022.104029

General rights

Copyright and moral rights for the publications made accessible in the public portal are retained by the authors and/or other copyright owners and it is a condition of accessing publications that users recognise and abide by the legal requirements associated with these rights.

- Users may download and print one copy of any publication from the public portal for the purpose of private study or research.
 You may not further distribute the material or use it for any profit-making activity or commercial gain
 You may freely distribute the URL identifying the publication in the public portal -

If you believe that this document breaches copyright please contact us at vbn@aub.aau.dk providing details, and we will remove access to the work immediately and investigate your claim.

Downloaded from vbn.aau.dk on: November 15, 2025

Multi-objective Stochastic Planning of Electric Vehicle Charging Stations in Unbalanced Distribution Networks Supported by Smart Photovoltaic Inverters

Khalil Gholami¹, Shahram Karimi^{2,*}, Amjad Anvari-Moghaddam³

¹Department of Electrical Engineering, Kermanshah Branch, Islamic Azad University, Iran (kgholami212@gmail.com).

^{2,*}Department of Electrical Engineering, Razi University, Kermanshah, Iran.

Abstract

Due to the environmental concerns, getting deteriorated ongoingly, it is becmoing essential to encourage people to use sustainable energies. One of the most effective alternatives to mitigate pollution is to promote green mobility via electric vehicles (EVs). However, the lack of electric charging stations (EVCS) may decrease individuals' satisfaction to use EVs in daily life. To bridge the gaps, this paper aims to simultaneously allocate EVCS and smart photovoltaic inverters (SPIs) in distribution networks to optimize three important objetive functions, including power loss, voltage deviation (VD), and voltage unbalance factor (VUF). To solve such a multi-objective optimization problem, a novel hybrid fuzzy Pareto dominance concept with differential evolution algorithm (FPDEA) is proposed to identify non-dominanted solutions. For practical considerations, the uncertainty of loads is also captured using Monte Carlo Simulations (MCSs). The effectiveness of the stochastic multi-objective approach is then examined and verified on an unbalanced 37-bus network under different case studies. Attained results illustrate that EVCSs can be effectively integrated into networks where SPIs are installed and able to support ancillary services (e.g., reactive power compnesation).

Keywords: Electric vehicle, unbalanced distribution networks, unbalanced voltage compensation, smart PV inverters, multi-objective optimization.

³ Department of Energy (AAU Energy), Aalborg University, 9220 Aalborg, Denmark.

1. Introduction

Electric vehicles (EVs) are indeed a convenient option for transportation systems due to pressure from carbon dioxide emissions, environmental degradation, and energy shortages. Nevertheless, limitted number of charging stations is also becoming a significant impediment to the broad adoption of EVs. Moreover, the global fleet market for EVs is growing imposing new challenges to the power systems operators in terms of peak load mamagement, and frequency and voltage regulations, among others [1].

So far, various investigations have been done to optimally allocate EV charging stations (EVCSs) in balanced distribution networks. Authors in [2] proposed a stochastic approach based on a point estimation model to find out the optimal location and sizing of charging stations for EVs. The objective function was the summation of several objective functions, e.g., the cost of purchasing land, the cost of facilities for establishing EV stations, maintenance costs, etc. The problem was then solved via a genetic algorithm. Similarly, in [3], EVCSs were determined by a teaching-learning based optimization (TLBO) algorithm to consider three objective functions, including real power loss, voltage deviation index, and voltage stability index. All these functions were combined via three coefficient (weighted-sum approach) and were implemented on two balanced distribution networks, namely 33 and 69 buses. In addition, EVCSs considering capacitor banks and distributed generations were allocated in balanced distribution grids via the genetic algorithm in [4]. Power losses minimization by placing EVCSs and DGs was also addressed in balanced distribution grids in [5]. Similarly, in [6], a bi-objective planning approach, e.g., energy cost and emission, was developed to allocate EVCSs, renewable energies, and energy storage in distribution grids. The model was solved by multi-objective particle swarm optimization and was implemented in a case study in China. A comprehensive assessment of the advantages of EVCSs and renewable energies was also investigated in [7]. Authors of [8] used a planning approach for EVCSs, and distributed generation in balanced distribution networks via three heuristic algorithms. A hybrid approach based on the genetic and particle swarm optimization algorithms was developed in [9] to optimize several objective functions, including power losses, voltage deviation, the cost of charging and load, and the cost of an EV battery. EVCSs and capacitor banks were placed in distribution networks to alleviate of the power loss, maximize

the network's benefit, and reliability enhancement in [10]. All these investigations were concentrated on balanced distribution systems and the properties of unbalanced networks have not been taken into account. However, distribution networks are inherently unbalanced, so EVCSs at various loading rates drastically affect voltage regulation, transformer loading, and power flows through different phases of distribution grids. When EVCSs are connected in an unsettling form among different phases, nodal voltages, line currents, active and reactive powers, and energy loss might get changed and deteriorated from what initially calculated/planned [11, 12]. Under real conditions, the distribution systems may be unbalanced which has some drawbacks compared to balanced networks, like more power losses, equipment malfunction, etc. Several research efforts have been focused on unbalanced networks to prevent such a problem. For instance, in [13], the authors elaborated on the allocation of EVCSs and distributed generations in unbalanced systems. The objective function was power loss minimization and solved via particle swarm optimization algorithm. Similarly, authors in [14], proposed a multi-objective planning of EVCSs in unbalanced distribution networks, considering several objective functions, such as minimizing the annualized investment cost, system losses, voltage deviation, etc. However, unbalanced voltage compesation and reactive power capability of smart inverters were not considered in that study. In [15], a modified version of the dragonfly algorithm was proposed for power loss minimization of distribution networks, where the impact of demand increase in some phases of network was investigated on voltage unbalance. However, unbalanced voltage compensation was not considered as an objective function.

As clearly seen from the reviewed literature, there are still some gaps needing further investigations. Firstly, most of the previous works have been focused on balanced electrical systems while in practice, operators deal with many unbalanced conditions. Although some efforts have been made on unbalanced networks, they did not consider abilities of photovoltaic (PV) inverters in compensating the reactive power and voltage regulation which in turn increases system flexibility and decreases complexity in real-time operation.

Finally, the multi-objective stochastic procedure was framed without considering several important objective functions simultaneously from the viewpoint of distribution system operators, such as power loss, voltage unbalance, and voltage deviation. Accordingly, this paper tends to provide a comprehensive

planning of EVCSs in unbalanced networks while addressing the aforementioned issues. The contributions of the work are as follows:

- In the proposed study, EVCSs are allocated in unbalanced networks for decreasing power loss, voltage deviation (VD), and voltage unbalance factor (VUF).
- A multi-objective framework is developed based on the hybridizing fuzzy Pareto dominance with differential evolution algorithm (FPDEA) to recognize a set of non-dominated solutions. A compromised solution is finally selected based on the fuzzy rules.
- The reactive power capabilities of smart PV inverters (PSIs) are also deployed as an ancillary service to support system when EVCs are integrated into networks. The advantage of this solution compared to conventional ones are demonstrated in several case studies.
- To capture realistic working conditions, uncertainty of load is also modeled via Monte Carlo simulations (MCSs).

2. Smart inverters

Conventionally, PV inverters were developed for converting the DC solar power to AC active power at unity power factor. However, distribution system operators or solar farm owners tend to get inverters' potential to absorb or inject reactive power into the system. To put it differently, when transforming DC electricity from PV panels to AC real power, the inverters' capacities are not deployed entirely. Reactive power could therefore be compensated by employing the inverter's unused capacity. To illustrate that, an example is shown in Fig.1. The amount of generated reactive power can be specified by the 4 point characteristics (A1-A4). The first segment of the curve (before point A1) denotes a condition where the maximum amount of injected reactive power (into the grid) has been reached. The next segment (from point A1 to point A2), denotes the ability to inject reactive power into the network by the inverter. The region between points A2 and A3 is described as the dead band range, in which the reactive power is neither injected to nor absorbed from the system. The last segment (between points A3 and A4) shows the ability of an inverter to absorb reactive power till the maximum capacity is reached. In this investigation, the rating

of smart PV inverters is calculated to support the unbalanced distribution network under different loading conditions which is mainly affected by EVs charging demands.

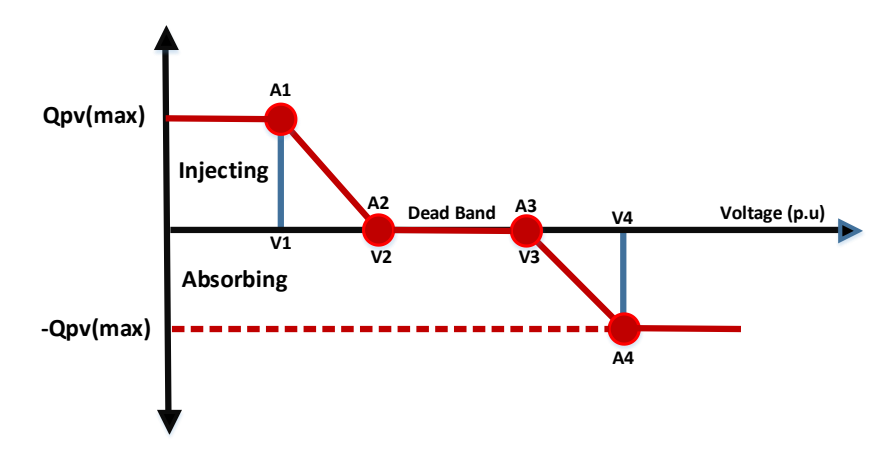


Fig. 1 the characteristic of smart PV inverter to support the reactive powers

3. Problem formulation

3.1. Objective functions

Three objective functions are considered in this paper as discussed in the following.

3.1.1. Power loss

Generally, 5-10 percent of the entire energy produced in electricity grids is lost at the distribution side [16]. High energy losses in distribution networks could give rise to equipment deterioration due to overheating [17]. To this end, line losses reduction in distribution networks is considered as the first objective in this work.

$$SLoss_{a,b,c}^{ij} = (V_{a,b,c}^{i} - V_{a,b,c}^{j})(I_{a,b,c}^{ij})^{*}$$
 (1)

$$PLoss_{a,b,c}^{ij} = real\left(SLoss_{a,b,c}^{ij}\right) \tag{2}$$

in above, $SLoss_{a,b,c}^{ij}$, and $PLoss_{a,b,c}^{ij}$ denote the complex, and real power losses, respectively; $V_{a,b,c}^{i}$ and $V_{a,b,c}^{j}$ are voltages of buses i and j, respectively; $I_{a,b,c}^{ij}$ shows the current of line ij.

$$Obj 1 = \min\left(\sum_{m} PLoss_{a,b,c}^{ij}\right)$$
(3)

3.1.2. Voltage deviation

The goal of this fitness function is to maximize the voltage at all nodes of the network by reducing the difference between the voltage of the slack node and the voltage of the *i*th node. It results in a flatter voltage profile across the network, which reduces under voltage at feeders located too far from the substation. The voltage deviation decrease is given as the second objective function as follows [18]:

$$VD^{i} = \left| V_{a,b,c}^{sub} - V_{a,b,c}^{i} \right| \tag{4}$$

here, $V_{a,b,c}^{sub}$ and $V_{a,b,c}^{i}$ are the voltages of the substation and nodes for three phases.

The second objective function is eventually modeled by the following equation.

$$Obj \ 2 = \min\left(\sum_{i} VD^{i}\right)$$
 (5)

3.1.3. Voltage unbalance factor

Unbalanced voltage compensation is one of the most important objective functions for electrical distribution system operation and planning. This is because a significant portion of consumers are linked to single-phase of networks, resulting in voltage imbalance in the system. Similarly, in unbalanced distribution systems, EVCSs are distributed across multiple phases, affecting the voltage of other buses through the network. As a result, when EVCSs are placed at the single-phase network, VUF should be considered as an objective function. The following relation expresses VUF [12]:

$$VUF^{i} = \left| \frac{V_{neg}^{i}}{V_{pos}^{i}} \right| \times 100 \tag{6}$$

In distribution systems, rising electricity supply varies the voltage levels, resulting in negative or positive voltage sensitivity. The Fortescue transform is used to determine the positive and negative voltage sequences as follows [19]:

$$V_{neg}^{i} = \frac{V_a^{i} + a^2 V_b^{i} + a V_c^{i}}{3} \tag{7}$$

$$V_{pos}^{i} = \frac{V_{a}^{i} + aV_{b}^{i} + a^{2}V_{c}^{i}}{3}$$
 (8)

$$a = 1 \angle 120^{\circ} \tag{9}$$

where, V_{neg}^{i} and V_{pos}^{i} respectively signify the negative and positive voltage sequences at the *ith* node; V_{a}^{i} , V_{b}^{i} , and V_{c}^{i} denote the voltages of phases a, b, c, respectively. Finally, the third objective function, VUF, is defined as follows:

$$Obj 3 = \min\left(\sum_{i} VUF^{i}\right)$$
(10)

3.2. Operational constraints

Following constraints are used to secure operation of the system under the planning of EVCSs. The constraints (11) is used to keep voltage within acceptable ranges; in (12), the line current capacity is enforced; equations (13) and (14) are representing the active and reactive power capacity of PV resources; the size of EVCSs could be then limited between its maximum and minimum values via (15) and (16).

$$V_{a,b,c}^{\min} \le V_{a,b,c}^{i} \le V_{a,b,c}^{\max} \tag{11}$$

$$I_{a,b,c}^{ij} \le I_{a,b,c}^{\max} \tag{12}$$

$$PV_{a,b,c}^{\min} \le PV_{a,b,c}^{k} \le PV_{a,b,c}^{\max} \tag{13}$$

$$QPV_{a,b,c}^{\min} \le QPV_{a,b,c}^{k} \le QPV_{a,b,c}^{\max} \tag{14}$$

$$PEVCS_{a,b,c}^{\min} \le PEVCS_{a,b,c}^{l} \le PEVCS_{a,b,c}^{\max}$$
(15)

$$QEVCS_{a,b,c}^{\min} \le QEVCS_{a,b,c}^{l} \le QEVCS_{a,b,c}^{\max}$$
(16)

here, $V_{a,b,c}^{\min}$ and $V_{a,b,c}^{\max}$ denote the maximum and minimum permissible voltages, respectively. $I_{a,b,c}^{ij}$ and $I_{a,b,c}^{\max}$ are the line current and its maximum capacity, respectively. $PV_{a,b,c}^{\min}$ and $PV_{a,b,c}^{\max}$ respectively show the maximum and minimum active rating of PVs. $QPV_{a,b,c}^{\min}$ and $QPV_{a,b,c}^{\max}$ respectively show the maximum

and minimum reactive rating of smart PV inverters. $PEVCS_{a,b,c}^{\min}$ and $PEVCS_{a,b,c}^{\max}$ denote the minimum and maximum capacities of active demand of EVCSs. $QEVCS_{a,b,c}^{\min}$ and $QEVCS_{a,b,c}^{\max}$ illustrate the minimum and maximum capacities of reactive demand of EVCSs.

4. Scenario generation

Uncertainties play the prominent role in the operation and planning of power systems. To model the uncertain parameters, a proper probability density function (PDF) is considered initially. Every PDF is then separated into multiple segments, i.e. a normal PDF with seven components is illustrated in Fig.2. As can be seen, every probability level indicates a particular error in the parameter under uncertainty. The procedure of scenario creation is accompanied by deploying a roulette wheel mechanism (RWM). For each uncertain variable, a number is randomly generated in the interval [0, 1]. This random number falls into one of the probability levels of the PDF. This approach is repeated until a set of scenarios are generated [20, 21].

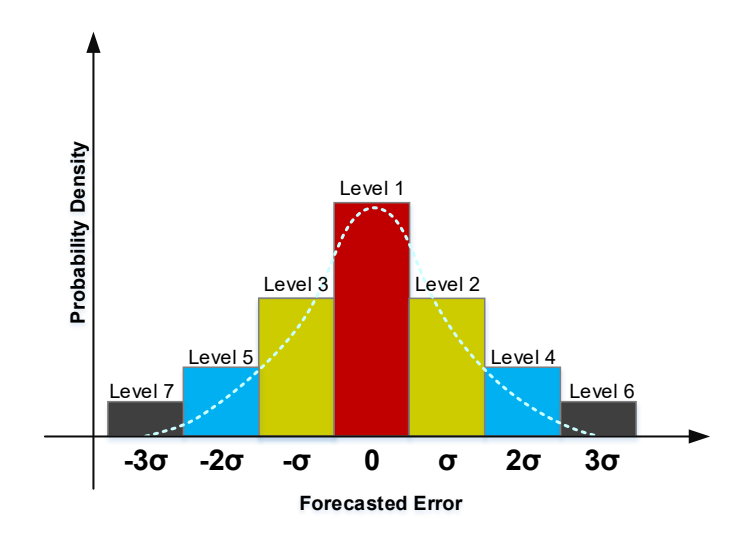


Fig. 2 a sample of normal PDF

5. Optimization process

As a heuristic approach, the differential evolution (DE) method is capable of solving non-deterministic polynomial-time challenging tasks. This method was created to address the fundamental disadvantage of the genetic algorithm, which is its lack of local search. There are four critical steps in this procedure. At the

beginning, this approach creates the population between the upper and lower limits of problems. The function called mutation is then employed to produce a new member regarding selecting several individuals in the population. The mutant individual is then joined with the *i*th member of the population through the crossover operator. By getting operators mentioned above, a new member is created and assessed according to the objective function. This individual's fitness is matched against the fitness of the corresponding individual, and the best one is chosen for the coming generations. It is noted that these processes are performed until the terminating conditions are fulfilled. The preceding procedure shows these steps [22, 23].

5.1. Initialization

Within the problem's search space, the population is produced probabilistically as follows:

$$W_{n,m} = LB_{n,m} + (UB_{n,m} - LB_{n,m}) * rand_1 \quad for \quad n = 1, 2, ..., NP \quad \& \quad m = 1, 2, ..., NV$$
 (18)

where W denotes the problem's decision variables; The terms NP, UB, and LB signify the population size, as well as the upper and lower boundaries; rand1 is a number with a consistent value between 0 and 1; The number of variables is represented by NV.

5.2. Mutation operator

Since one new solution is developed via existing individuals, this phase is the most crucial segment of the DE process. Three members of the population are picked at random, and a new solution named X_n^{G+1} is generated by:

$$X_n^{G+1} = W_{r_1}^G + F_c * (W_{r_2}^G - W_{r_3}^G)$$
(19)

 F_c in the above expression is a fixed value in the range [0, 2]. Furthermore, the three parameters picked at random are expressed by W_{r1}^G , W_{r2}^G and W_{r3}^G .

5.3. Crossover operator

The new solution, which was previously created during the mutation stage, is now blended with the population's *i*th member to increase its variety. A solution that allows escaping from local optimal solution is created based on the solution obtained from the mutation operator and the *n*th member of the population.

$$Y_{n,m}^{G+1} = \begin{cases} X_{n,m}^{G+1} & \text{if } rand_{2} \leq C_{r} \text{ or } m = m_{rand} \\ W_{n,m}^{G} & \text{otherwise} \end{cases}$$
(20)

The Y_n^{G+1} solution is constructed using the W_n^G and X_n^{G+1} , as well as the C_r term (a user-selected number between zero and one). m_{rand} is a uniform random number ranging from [0 1].

5.4. Selection operator

The desired solution is saved for next generation in this stage. It means if the efficiency of the produced member, that is, Y_n^{G+1} , is better than the *n*th individual in the population, it will be retained for the next generation; conversely, the preceding member, i.e., W_n^G will be kept for the next generation.

$$W_{n}^{G+1} = \begin{cases} Y_{n}^{G+1} & \text{if fitness}\left(Y_{n}^{G+1}\right) \leq \text{fitness}\left(W_{n}^{G}\right) \\ W_{n}^{G} & \text{otherwise} \end{cases}$$

$$(21)$$

here, $fitness(\cdot)$ refers to the fitness values of the underlying solutions.

5.5. Fuzzy Pareto dominance

Even though the mentioned DE algorithm can be either used to solve a single objective function or utilized for solving multi-objective functions by combining multiple objectives into just one objective is easier to use for tackling optimization problems, it is incapable of identifying alternate solutions. The Pareto-dominance technique is a subclass of metaheuristic algorithms that gives a broader variety of possible solutions, resulting in greater flexibility in decision-making. Specific methods, for instance, may result in a more significant quality enhancement in voltage deviation, whereas others result in improved compensation for voltage imbalance. Because multiple solutions are available, the operator can select the solution that enhances the indices depending on the system status [24–26].

The fuzzy Pareto dominance (FPD) approach is used in this research to identify the non-dominated solutions by the DEA. Mathematically explaining, a solution, here f1, is dominated by another solution, e.g., f2, at the degree of μp is given as:

$$\mu p(f 1, f 2) = \frac{\prod_{i} \min(f 1_{i}, f 2_{i})}{\prod_{i} f 2_{i}}$$
(22)

in which f1 and f2 are indeed the fitness values of the two selected solutions. The amount of domination ranges from 0 to 1. If it is equal to 1, f2 completely dominates f1. The solutions are non-dominated if $\mu p(f 1, f 2)$ and $\mu p(f 1, f 2)$ are both smaller than 1.

After identifying the non-dominant solutions, selecting one of the solutions is required. To accomplish so, the list of solutions is normalized into ranges between zero and one as shown.

$$\mu_{fi}(W) = \begin{cases} \frac{1}{fitness_{i}^{\max} - fitness_{i}(W)} & fitness_{i}^{\min}(W) \leq fitness_{i}^{\min} \\ fitness_{i}^{\max} - fitness_{i}^{\min} & fitness_{i}^{\min} < fitness_{i}(W) < fitness_{i}^{\max} \\ 0 & fitness_{i}^{\min}(W) \geq fitness_{i}^{\max} \end{cases}$$

$$(23)$$

The ith function's minimum and maximum fitness are indicated by $fitness_i^{min}$ and $fitness_i^{max}$, respectively. Using the following criteria, the final solution is chosen from among the normalized solutions:

$$\gamma_{\mu}(n) = \frac{\sum_{i=1}^{N_{of}} C_{i} \times \mu_{fi}(x_{n})}{\sum_{m=1}^{N_{r}} \sum_{i=1}^{N_{of}} C_{i} \times \mu_{fi}(x_{n})}$$
(24)

In the above equation, N_r denotes the number of solutions in the repository, and μ_{fi} means the normalized fitness function for the nth solution. Furthermore, the weighting coefficient is represented by the parameter C_i .

The procedure of mentioned optimization approach is illustrated in Fig.3.

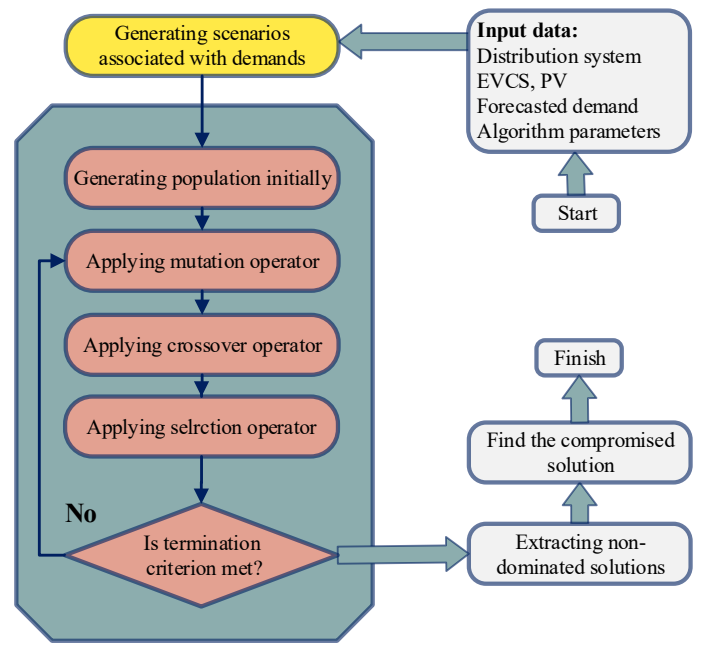


Fig.3 the flowchart of the proposed optimization procedure

6. Simulation results

A modified 37-bus unbalanced distribution network shown in Fig. 4 is used as a test system to verify the applicability of the proposed method [27]. This is a real test system corresponding to an underground network in California. Bus 1 is selected as the slack bus and base voltage is 4.8kV. Comparing to the original 37-bus network, some voltage regulators were removed and replaced by lines. The data of test system is provided in Appendix. It is assumed that a three-phase EVCS which the capacity of each phase is 100kW and 100kVAr is candidate to be allocated into the network. Despite those, three three-phase SPIs are also considered to be assigned to the system. Also, the uncertainty of loads have direct effect on planning and operation schemes. Accordingly, the uncertainty of load should be modeled for making a robust decision under such circumstances. To this end, some errors are added into the forecasted values (see Table 1 in appendix) to generate the load scenarios based on the procedure discussed in section 4. The generated load scenarios are illustrated in Fig. 5. The proposed approach is then evaluated under the following cases.

- Case 1: base case without any resources
- Case 2: merely EVCSs allocation
- Case 3: merely SPIs allocation
- Case 4: both EVCSs and SPIs allocations

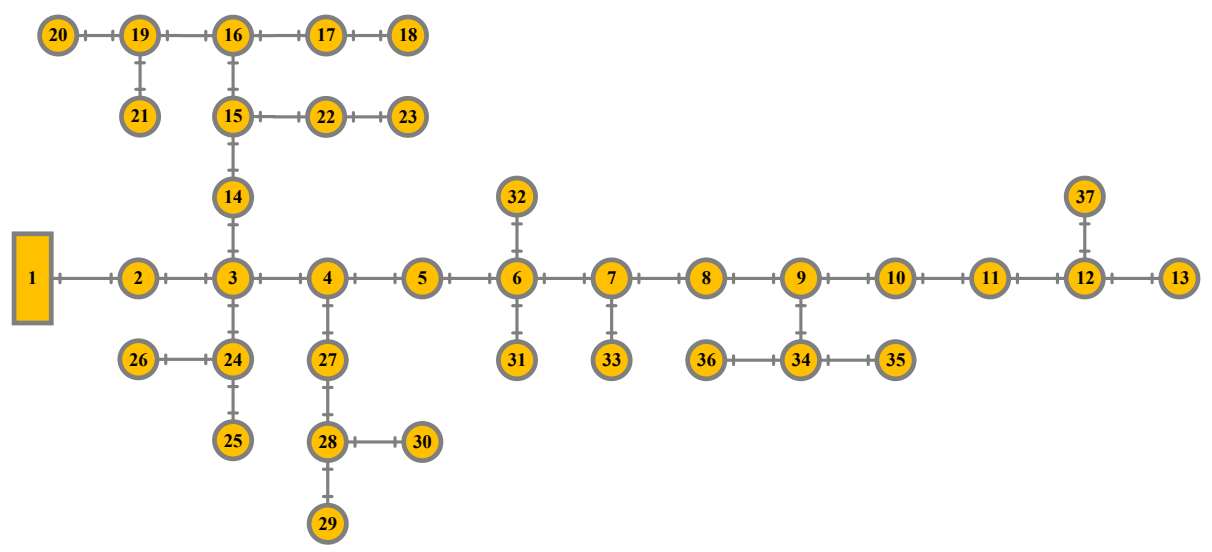


Fig.4 the line diagram of 37-bus unbalanced distribution grid

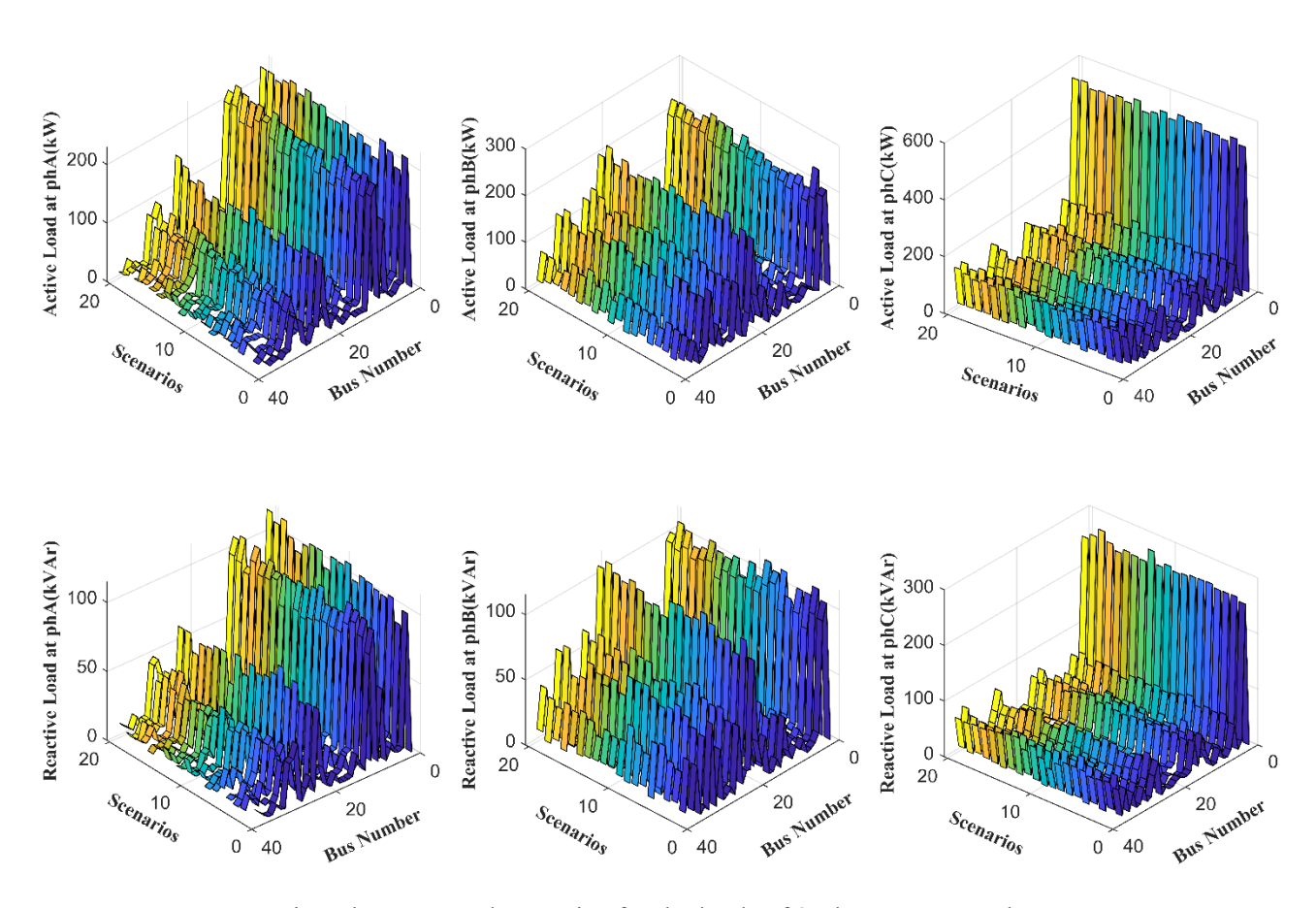


Fig.5 the generated scenarios for the loads of 37-bus test network.

As can be seen from Fig. 6, the power loss of the system varies from 300 to 350 kW in case 1 depended on load scenarios. However, it is increased if EVCS is integrated in case 2, where the power loss is between 400 to 480. This trend decreases effectively when SPIs are installed in the system in case 3. On the other hand, in case 4 where EVCS and SPIs co-exist, the power loss has a slightly different pattern, meaning that SPIs contribute in the power loss minimization while EVCS impose additional power loss into the system. From this comparison, it is clear that SPIs can compensate for the power loss imposed into the system.

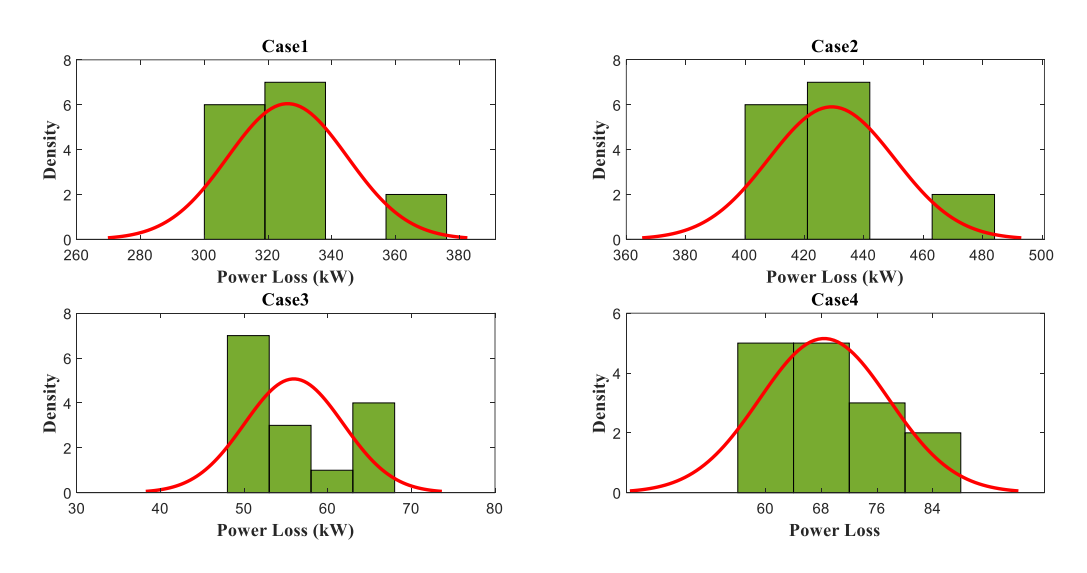


Fig.6 the power loss of the network

Fig. 7 illustrates the voltage deviation of system under 4 cases. The total voltage deviation (*Obj 2*) in case 1 is approximately between 7.4 p.u and 8.2 p.u. However, it accounts for between 8.6 p.u and 9.4 p.u in case 2, which is higher than case 1. Surprisingly, it varies from 1.5 p.u to 2.2 p.u, when SPIs were allocated to network. Consequently, in case 4 where EVCS and SPIs are installed, there is also a significant decrease in voltage deviation, even compared to case 1. Accordingly, simultaneous integration of EVCS and SPIs can be an excellent remedy to support the system and decrease voltage violations.

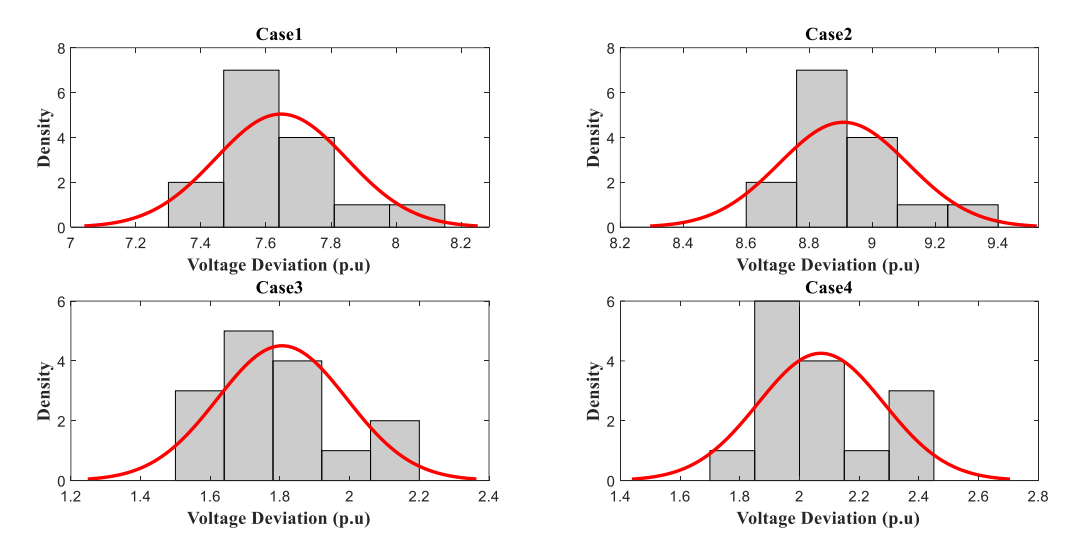


Fig.7 the voltage deviation of the network

Unbalanced voltage compensation is also an essential factor when planning EVCSs. The VUF for all cases is depicted in Fig. 8. It should be noted that these values are the summation of VUF across the network (*Obj 3*). As clearly seen, the VUF is the highest in case 2, where EVCS is integrated to the network. However, a significant decrease is witnessed in Case 3 due to the allocation of SPIs. In other words, this reaches the least VUF in case 3. Finally, in case 4, the amount of VUF is more minor than case 1 and 2, although there is a slight increase compared with case 3. This comparison shows that the amount of VUF decreases, if SPIs cooperate in supporting system.

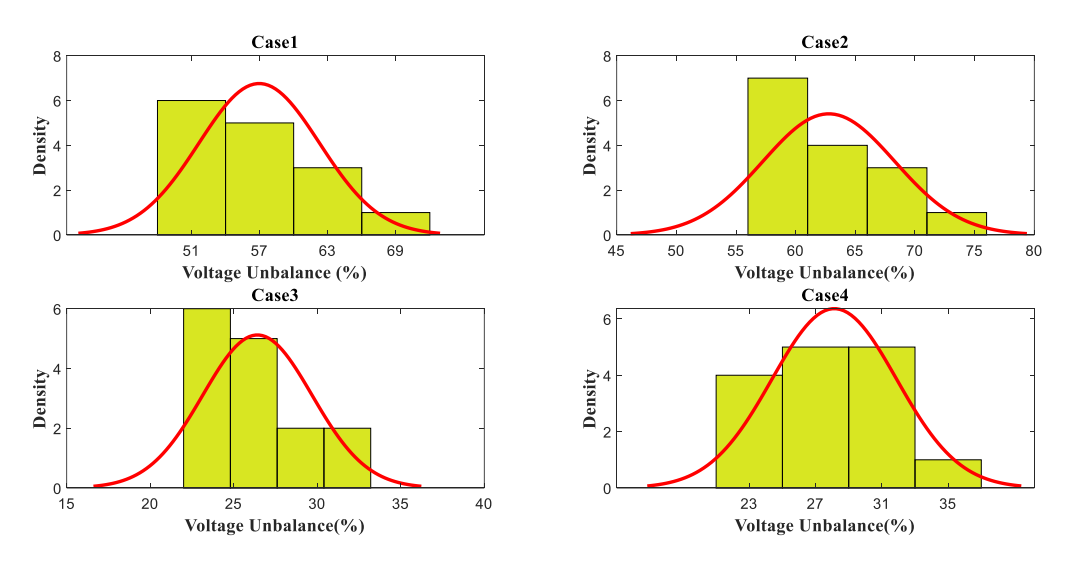


Fig.8 the voltage unbalance factor of the network

The PDFs of active power generated by PVs in cases 3 and 4 are revealed in Fig. 9. In more detail, as mentioned above, the three three-phase SPIs are allocated into network. For example, active power of PV1 is the amount of generated power by PV1 which is injected to phase A, B, and C. As can be seen, the active power generated by PVs in case 3 is less than in case 4. This is because a significant consumption is supported by PVs. However, the consumption of network has a little increased by EVCS, so the generation of PVs increases slightly.

Fig. 10 depicts the PDFs for reactive power generation of PVs for cases 3 and 4. Similarly, the reactive powers in case 4 which PVs must generate are higher than case 3. As explained above, there is reactive power penetration in networks via EVCS in case 4. PVs, on the other hand, could participate in supporting reactive power by smart inverters.

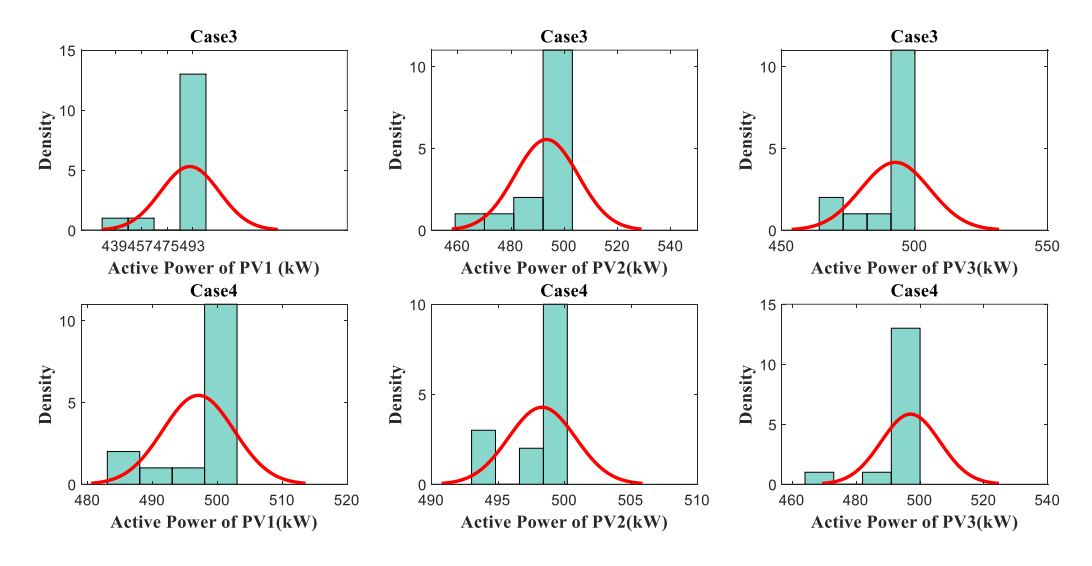


Fig.9 the active power generation of PVs in cases 3 and 4

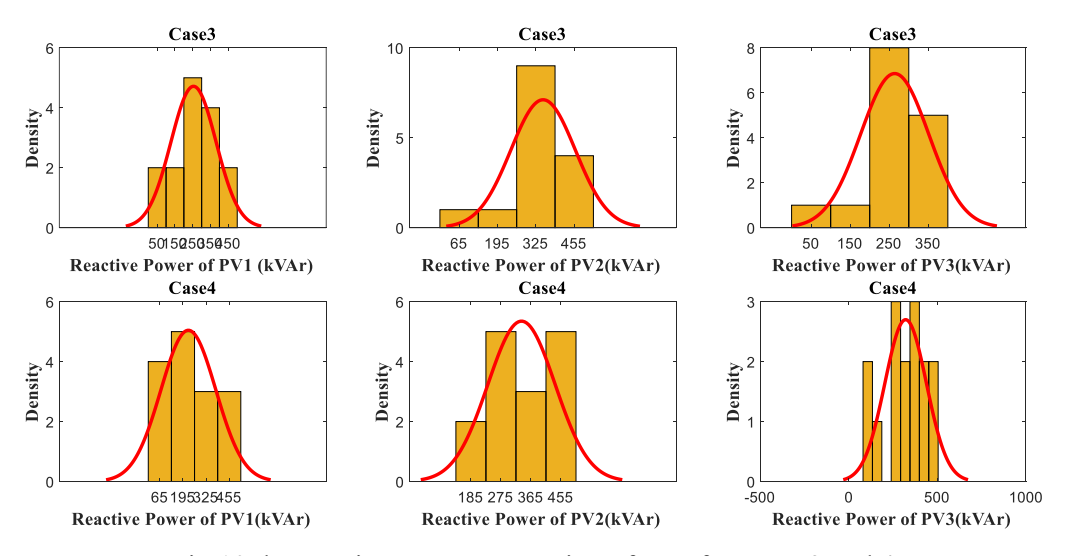


Fig. 10 the reactive power generation of PVs for cases 3 and 4

In the Fig.11, there are possible locations for different resources in all cases. In other words, a set of locations are obtained after solving the problem for various scenarios. A number of scenarios lead to different loacations. To find optimal locations to allocate resources, the most repeated locations should be selected. According this, the optimal location can be recognized. The optimal location and capacities for resources are finally shown in Table 1, which are extracted based on Fig.11.

The voltage profile of the network per each phase is depicted in Fig. 12. It is clear that, when EVCS is integrated in the system, voltage at all phases decreases. However, it can be enhanced by PV inverters as shown in case 3 and 4.

At each bus, the VUF is illustrated in Fig.13. The amount of VUF decrees significantly in case 3, where just PVs are allocated. However, it reaches the summit in case 2, where EVCS is allocated into the network. On the other hand, simultaneous integration of EVCS and SPIs, case4, helps to keep this factor under expected value.

Table 1. The results obtained based on the different scenarios

Case No.	Obj1 (kW)	Obj2 (p.u)	Obj3 (%)	EVCS location	EVCS Capacity	SPIs location	SPIs Capacity
Case1	196.87	5.80	43.11	-	-	-	-
Case2	220.62	6.21	44.74	Phase ABC: 3	Phase ABC: 100kW, 100kVAr	-	-
Case3	53.87	1.82	20.86	-	-	PV1: PhaseABC:14 PV2: PhaseABC: 4 PV3: PhaseABC:9	PV1: Phase ABC:500 kW, 195 kVAr PV2: Phase ABC:500 kW, 325 kVAr PV3: Phase ABC: 500kW, 250 kVAr
Case4	49.56	1.71	22.57	Phase ABC: 3	Phase ABC: 100kW, 100kVAr	PV1: PhaseABC:10 PV2: PhaseABC:4 PV3: PhaseABC:15	PV1: Phase ABC:500 kW, 195 kVAr PV2: Phase ABC:500 kW, 275 kVAr PV3: Phase ABC:500 kW, 265 kVAr

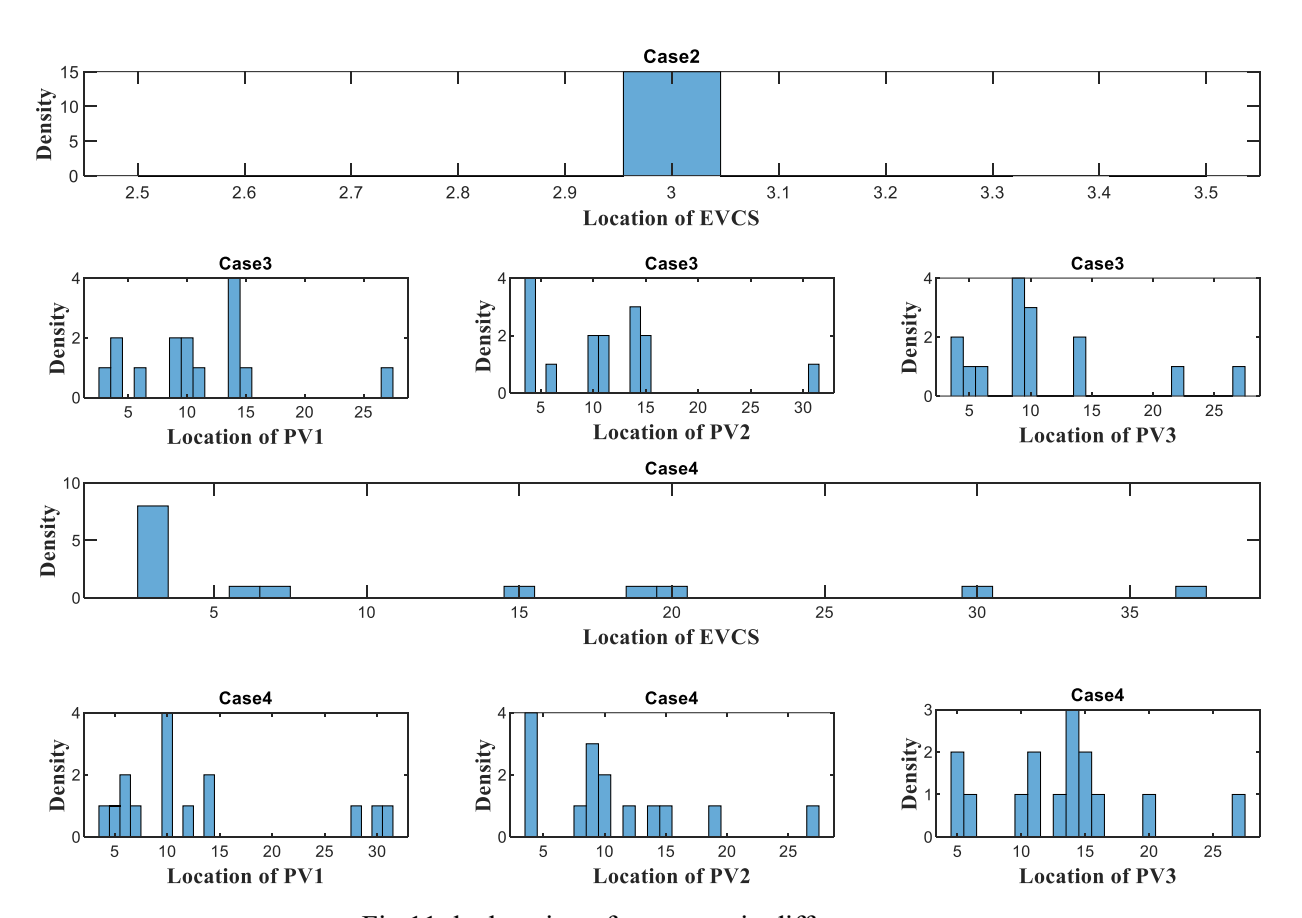


Fig.11 the location of resources in different cases

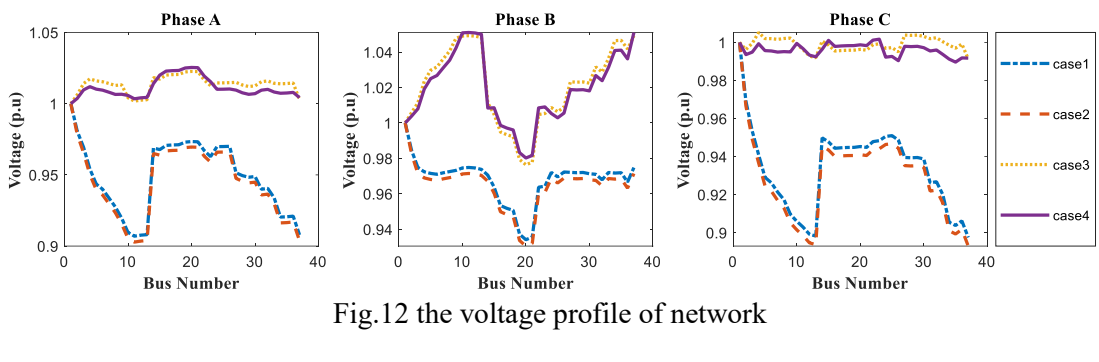


Fig.13 the VUF at each bus of network

7. Conclusion

In this paper, smart photovoltaic inverters have been deployed as means of ancillary service to support extra demand imposed to the network via allocating EVCSs. The proposed planning of EVCSs was formulated as a stochastic multi-objective framework based on a hybrid fuzzy dominance concept with a differential evolution algorithm. The performance of planning approach was studied on an unbalanced network under four different cases, including base case, just EVCS allocation, merely SPIs sizing and placement, and simultaneous EVCS and SPIs integration. Simulations results demonstrated that EVCS could impose various challenges into the network such as the increase in power loss, voltage deviation, and voltage unbalance. However, it could be seen that, such problems can be tackled if SPIs are appropriately designated into the system. Accordingly, SPIs were deemed as a promising remedy to compensate the voltage imbalance, voltage profile enhancement, and power loss reduction. In sequel investigations, power quality issues would be considered when EVCSs are integrated into the unbalanced networks.

Appendix

Table A. the data of modified 37-bus unbalanced distribution network

Branch Number	Sending End	Receiving End	Conductor type	Length (ft)	Demand at receiving end of Phase A (kVA)	Demand at receiving end of Phase B (kVA)	Demand at receiving end of Phase C (kVA)
1	1	2	1	1850	210 + 105j	210 + 105j	525 + 262.5j
2	2	3	2	960	0.00 + 0.00j	189 + 93.0j	0.00 + 0.00j
3	3	4	2	1320	0.00 + 0.00j	0.00 + 0.00j	0.00 + 0.00j
4	4	5	3	600	0.00 + 0.00j	0.00 + 0.00j	127.5 + 60.0j
5	5	6	3	200	0.00 + 0.00j	0.00 + 0.00j	0.00 + 0.00j
6	6	7	3	320	0.00 + 0.00j	0.00 + 0.00j	0.00 + 0.00j
7	7	8	3	320	127.5 + 60.0j	0.00 + 0.00j	0.00 + 0.00j
8	8	9	3	560	0.00 + 0.00j	0.00 + 0.00j	63.0 + 31.5j
9	9	10	3	640	210 + 105j	0.00 + 0.00j	0.00 + 0.00j
10	10	11	3	400	189 + 93.0j	0.00 + 0.00j	0.00 + 0.00j
11	11	12	3	400	0.00 + 0.00j	0.00 + 0.00j	31.5 + 15.0j
12	12	13	3	400	0.00 + 0.00j	63.0 + 31.5j	63.0 + 31.5j
13	3	14	3	360	0.00 + 0.00j	0.00 + 0.00j	127.5 + 60.0j
14	14	15	3	520	0.00 + 0.00j	0.00 + 0.00j	31.5 + 15.0j
15	15	16	3	800	0.00 + 0.00j	0.00 + 0.00j	127.5 + 60.0j
16	16	17	3	600	0.00 + 0.00j	0.00 + 0.00j	0.00 + 0.00j
17	17	18	4	280	0.00 + 0.00j	63.0 + 31.5j	0.00 + 0.00j
18	16	19	4	920	0.00 + 0.00j	0.00 + 0.00j	0.00 + 0.00j
19	19	20	4	760	0.00 + 0.00j	63.0 + 31.5j	0.00 + 0.00j
20	19	21	4	120	0.00 + 0.00j	210 + 105.j	31.5 + 15.0j
21	15	22	4	80	25.5 + 12.0j	31.5 + 15.0j	0.00 + 0.00j
22	22	23	4	520	127.5 + 60.0j	0.00 + 0.00j	0.00 + 0.00j
23	3	24	4	400	0.00 + 0.00j	0.00 + 0.00j	0.00 + 0.00j
24	24	25	4	320	12.0 + 6.00j	127.5 + 60.0j	0.00 + 0.00j
25	24	26	4	240	0.00 + 0.00j	0.00 + 0.00j	127.5 + 60.0j
26	4	27	4	240	0.00 + 0.00j	0.00 + 0.00j	63.0 + 31.5j
27	27	28	3	280	63.0 + 31.5j	0.00 + 0.00j	0.00 + 0.00j
28	28	29	4	280	63.0 + 31.5j	0.00 + 0.00j	0.00 + 0.00j
29	28	30	4	200	63.0 + 31.5j	63.0 + 31.5j	63.0 + 31.5j
30	6	31	3	0	0.00 + 0.00j	0.00 + 0.00j	0.00 + 0.00j

31	6	32	3	600	0.00 + 0.00j	127.5 + 60.0j	0.00 + 0.00j
32	7	33	4	320	0.00 + 0.00j	0.00 + 0.00j	63.0 + 31.5j
33	9	34	4	520	0.00 + 0.00j	0.00 + 0.00j	0.00 + 0.00j
34	34	35	4	200	0.00 + 0.00j	0.00 + 0.00j	127.5 + 60.0j
35	34	36	4	1280	0.00 + 0.00j	63.0 + 31.5j	0.00 + 0.00j
36	12	37	4	200	0.00 + 0.00j	0.00 + 0.00j	127.0 + 60.0j

Table B. the self and mutual impedances of lines (see Fig. A for more information)

G 1 . T	Impedance in ohms/mile							
Conductor Type	phase	a	b	С				
	a	0.2926+0.1973j	0.0673-0.0368j	0.0337-0.0417j				
1	b	0.0673-0.0368j	0.2646+0.1900j	0.0673-0.0368j				
	c	0.0337-0.0417j	0.0673-0.0368j	0.2926+0.1973j				
	a	0.4751+0.2973j	0.1629-0.0326j	0.1234-0.0607j				
2	b	0.1629-0.0326j	0.4488+0.2678j	0.1629-0.0326j				
	С	0.1234-0.0607j	0.1629-0.0326j	0.4751+0.2973j				
	a	1.2936+0.6713j	0.4871+0.2111j	0.4585+0.1521j				
3	b	0.4871+0.2111j	1.3022+0.6326j	0.4871+0.2111j				
	c	0.4585+0.1521j	0.4871+0.2111j	1.2936+0.6713j				
	a	2.0952+0.7758j	0.5204+0.2738j	0.4926+0.2123j				
4	b	0.5204+0.2738j	2.1068+0.7398j	0.5204+0.2738j				
	С	0.4926+0.2123j	0.5204+0.2738j	2.0952+0.7758j				

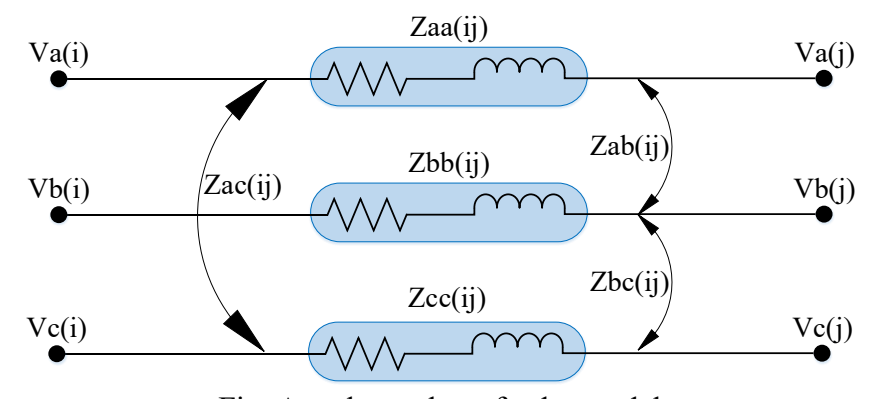


Fig. A. a three-phase feeder model

8. References

- 1. Saravanan, R., Kaliappan, S., Jayaprakasan, V., and Maniraj, P. (2022) A hybrid strategy for mitigating unbalance and improving voltage considering higher penetration of electric vehicles and distributed generation. *Sustain. Cities Soc.*, **76** (May 2021), 103489.
- 2. Mirzaei, M.J., Kazemi, A., and Homaee, O. (2016) A Probabilistic Approach to Determine Optimal Capacity and Location of Electric Vehicles Parking Lots in Distribution Networks. *IEEE Trans. Ind. Informatics*, **12** (5), 1963–1972.
- 3. Babu, P.V.K., and Swarnasri, K. (2020) Multi-objective optimal allocation of electric vehicle charging stations in radial distribution system using teaching learning based optimization. *Int. J. Renew. Energy Res.*, **10** (1), 366–377.
- 4. Pazouki, S., Mohsenzadeh, A., Ardalan, S., and Haghifam, M.R. (2015) Simultaneous Planning of PEV Charging Stations and DGs Considering Financial, Technical, and Environmental Effects. *Can. J. Electr. Comput. Eng.*, **38** (3), 238–245.
- 5. Jamian, J.J., Mustafa, M.W., Mokhlis, H., and Baharudin, M.A. (2014) Minimization of Power Losses in Distribution System via Sequential Placement of Distributed Generation and Charging Station. *Arab. J. Sci. Eng.*, **39** (4), 3023–3031.
- 6. Sun, B. (2021) A multi-objective optimization model for fast electric vehicle charging stations with wind, PV power and energy storage. *J. Clean. Prod.*, **288**, 125564.
- 7. Yang, M., Zhang, L., Zhao, Z., and Wang, L. (2021) Comprehensive benefits analysis of electric vehicle charging station integrated photovoltaic and energy storage. *J. Clean. Prod.*, **302**, 126967.
- 8. Sharma, P., Mishra, A.K., Mishra, P., and Dutt Mathur, H. (2021) Optimal Capacity Estimation and Allocation of Distributed Generation Units with Suitable Placement of Electric Vehicle Charging Stations. *TENSYMP 2021 2021 IEEE Reg. 10 Symp*.
- 9. Mozafar, M.R., Moradi, M.H., and Amini, M.H. (2017) A simultaneous approach for optimal allocation of renewable energy sources and electric vehicle charging stations in smart grids based on improved GA-PSO algorithm. *Sustain. Cities Soc.*, **32**, 627–637.
- 10. Bilal, M., and Rizwan, M. (2021) Integration of electric vehicle charging stations and capacitors in distribution systems with vehicle-to-grid facility. *Energy Sources, Part A*

- Recover. Util. Environ. Eff., $\mathbf{0}$ (0), 1–30.
- 11. Gray, M.K., and Morsi, W.G. (2016) Probabilistic quantification of voltage unbalance and neutral current in secondary distribution systems due to plug-in battery electric vehicles charging. *Electr. Power Syst. Res.*, **133**, 249–256.
- 12. Farahani, H.F. (2017) Improving voltage unbalance of low-voltage distribution networks using plug-in electric vehicles. *J. Clean. Prod.*, **148**, 336–346.
- 13. Reddy, M.S.K., and Selvajyothi, K. (2020) Optimal placement of electric vehicle charging station for unbalanced radial distribution systems. *Energy Sources, Part A Recover. Util. Environ. Eff.*, **0** (0), 1–15.
- 14. Kumar, N., Kumar, T., Nema, S., and Thakur, T. (2021) A multiobjective planning framework for EV charging stations assisted by solar photovoltaic and battery energy storage system in coupled power and transportation network. *Int. J. Energy Res.*, (August), 1–32.
- 15. Rajesh, P., and Shajin, F.H. (2021) Optimal allocation of EV charging spots and capacitors in distribution network improving voltage and power loss by Quantum-Behaved and Gaussian Mutational Dragonfly Algorithm (QGDA). *Electr. Power Syst. Res.*, **194** (September 2020), 107049.
- 16. Rizwan, M., Gholami, K., and Karimi, S. (2020) Optimal sizing and placement of the UPQC and DG simultaneously based on sensitivity analysis and firefly algorithm. *Int. J. Power Energy Convers.*, **11** (4), 1.
- 17. Murty, V.V.S.N., and Kumar, A. (2014) Capacitor allocation in unbalanced distribution system under unbalances and loading conditions. *Energy Procedia*, **54**, 47–74.
- 18. Li, C., Disfani, V.R., Haghi, H.V., and Kleissl, J. (2020) Coordination of OLTC and smart inverters for optimal voltage regulation of unbalanced distribution networks. *Electr. Power Syst. Res.*, **187** (July), 106498.
- 19. Ch, Y., Goswami, S.K., and Chatterjee, D. (2016) Effect of network reconfiguration on power quality of distribution system. *Int. J. Electr. Power Energy Syst.*, **83**, 87–95.
- 20. Kavousi-Fard, A., and Khodaei, A. (2016) Efficient integration of plug-in electric vehicles via reconfigurable microgrids. *Energy*, **111**, 653–663.

- 21. Hajiamoosha, P., Rastgou, A., Bahramara, S., and Bagher Sadati, S.M. (2021) Stochastic energy management in a renewable energy-based microgrid considering demand response program. *Int. J. Electr. Power Energy Syst.*, **129**, 106791.
- 22. Gholami, K., and Jazebi, S. (2020) Energy demand and quality management of standalone diesel/PV/battery microgrid using reconfiguration. *Int. Trans. Electr. Energy Syst.*, **30** (10), 1–21.
- 23. Gholami, K., and Jazebi, S. (2020) Multi-objective long-term reconfiguration of autonomous microgrids through controlled mutation differential evolution algorithm. *IET Smart Grid*, **3** (5), 738–748.
- 24. Asrari, A., Lotfifard, S., and Payam, M.S. (2016) Pareto Dominance-Based Multiobjective Optimization Method for Distribution Network Reconfiguration. *IEEE Trans. Smart Grid*, 7 (3), 1401–1410.
- 25. Jadidoleslam, M., Ebrahimi, A., and Latify, M.A. (2017) Probabilistic transmission expansion planning to maximize the integration of wind power. *Renew. Energy*, **114**, 866–878.
- 26. Köppen, M., Vicente-Garcia, R., and Nickolay, B. (2005) Fuzzy-Pareto-Dominance and its application in Evolutionary Multi-objective Optimization. *Lect. Notes Comput. Sci.*, **3410**, 399–412.
- 27. Montoya, O.D., Giraldo, J.S., Grisales-Noreña, L.F., Chamorro, H.R., and Alvarado-Barrios, L. (2021) Accurate and efficient derivative-free three-phase power flow method for unbalanced distribution networks. *Computation*, **9** (6), 1–21.